JOURNAL OF MATERIALS SCIENCE 14 (1979) 671–679

The decomposition of the solid solution state in the temperature range 20 to 200°C in an Al–Zn–Mg alloy

T. UNGÁR, J. LENDVAI, I. KOVÁCS
Loránd Eötvös University, Institut for General Physics, Budapest, Hungary

G. GROMA, E. KOVÁCS-CSETÉNYI
Research, Engineering and Prime Contracting Centre of the Hungarian Aluminium Corporation, Budapest, Hungary

The decomposition of the supersaturated solid solution of an Al–3.2 wt% Zn–2.2 wt% Mg alloy has been investigated in the temperature of 20 to 200° C, by small-angle X-ray scattering, electrical resistivity and mechanical measurements. On the basis of the results obtained, three subsequent stages of the decomposition process can be distinguished. Between 20 and 70° C the basic process is the nucleation and growth of G.P. zones, the volume fraction of which increases logarithmically with time. A transition stage is observed between 80 and 100° C in which the volume fraction increases linearly with time. Above 90° C, the growth kinetics of the volume fraction shows a definite incubation period at the beginning of ageing, while the yield stress increases monotonically. In the temperature range 100 to 160° C, the formation of the η' phase takes place. Below 100° C a linear connection between the yield stress and $(fR)^{1/2}$ is found from which the specific surface energy to cut a G.P. zone is calculated to be $\Gamma_0 = 0.21\ \mathrm{Nm\,m^{-2}}$.

1. Introduction

The process of zone formation and precipitation has been the subject of a number of investigations for the medium strength, weldable Al–Zn–Mg type alloys [1–6]. Below about 100° C the decomposition of the supersaturated solid solution state takes place basically by the formation of G.P. zones. At higher temperatures, roughly between 100 and 160° C, the partly coherent η' transition phase is being formed. At even higher temperatures, the precipitation of the η phase takes place with the composition of $MgZn_2$ and no coherency with the matrix. Several further equilibrium phases have been reported to exist above about 200° C in the medium strength Al–Zn–Mg alloy system but they play no role in the precipitation hardening of these alloys [1, 7].

Both the G.P. zones and η' phase are metastable particles in the alloy and, as such, are highly sensitive to the actual process of heat-treatment. The G.P. zones which are formed during long-term ageing at room temperature, become unstable at higher temperatures above about 100° C giving the well-known effect of reversion in Al–Zn–Mg alloys. The details of the temperature and time dependence of reversion have been reported in two previous papers for an Al–3.2 wt% Zn–2.2 wt% Mg alloy [8, 9].

Several investigations have shown that the nucleation and growth process of the η' transition phase is strongly dependent on whether or not the alloy was pre-aged at room temperature [4, 6]. The nucleation of the particles of η' is basically determined by the state of the alloy before the ageing process is started. The dispersity of the η' phase can be smaller by a factor of about three after a direct quenching to the ageing temperature compared to the dispersity obtained after a long pre-ageing at room temperature [4].

In the present paper, a systematic investigation

was carried out to study the decomposition of the supersaturated solid solution in the temperature range from room temperature to 200° C in an Al–3.2 wt % Zn–2.2 wt % Mg alloy.

2. Experimental

The investigations were carried out on an Al alloy containing 3.2% Zn, 2.2 % Mg, 0.25 % Si, 0.34 % Fe, 0.17 % Mn and 0.1 % Ti (all data in wt %). The process of decomposition was followed by the measurement of electrical resistivity, mechanical properties and small-angle X-ray scattering (SAXS). Electrical resistivity and the mechanical properties were measured on samples of 0.5 mm × 2.120 mm. SAXS measurements were carried out on thin foils 0.12 mm thick.

The samples were solution heat-treated at 480° C for 30 min in a vertical tube furnace and quenched into water at room temperature. Heat-treatments up to 100° C were carried out in a water bath and those between 100 and 200° C in a glycerine oil bath. The temperature of the liquid bath was constant to within ± 1° C.

Electrical resistivity measurements were carried out in liquid nitrogen by the usual potentiometric method. The mechanical properties were measured by an FM-250 type tensile test machine.

The SAXS experiments were carried out either in a Kratky type Anton-Paar camera, or in a Kiessing type AEG camera with a pin-hole collimation system. In the latter aparatus, the temperature of the sample could be kept constant to within ± 2° C up to ~500° C by a microfurnace. Owing to the low heat capacity of the microfurnace, a temperature lower than 200° C could be reached within 30 sec. This Kiessing type camera was modified in such a way that the integrated intensity (I.I.) scattered by the sample in the small-angle range between 0.5 and 3.5° in 2θ was detected by a scintillation counter. The modification of the camera was based on the work of Levelut and Guinier [10] and the details of it will be published elsewhere [11]. The signal of the scintillation counter was channelled through a differential discriminator and a linear rate meter.

The output signal of the rate meter was compensated by a constant potential of a stabilized potentiometer and only the change in the I.I. was registered on a plotter.

The intensity distribution of SAXS was determined by the Kratky camera with a scintillation counter by the usual step-by-step method. For both X-ray investigations, Cu$K\alpha$ radiation was used with Ni filtering and differential discrimination.

The intensity distribution curves were normalized to a scale by the application of a calibrated standard lupolen sample [11]. Numerical integration of the normalized intensity distribution curves yielded the volume fraction of the scattering particles in a similar way to that described in an earlier paper [9].

It is well known that the absolute value of the integral intensity in the small-angle range is strongly influenced by both the diffuse atomic scattering and the instrumental back-ground scattering [10, 12]. Both types of background scattering can distort somewhat the determination of the absolute value of the volume fraction of scattering particles. In the case of the alloy investigated here, this distortion yields a considerable relative error in the volume fraction especially in the initial (few hours) stage of the zone formation process, where, due to the relatively low content of Zn the increase of the scattered intensity is very small. This means that the kinetics of zone formation, at least at the beginning, can be followed by SAXS measurement only with a relatively high relative error. The scatters of measurements is probably further increased by the use of new samples for each state of ageing. This latter way of measurement was necessary, however, since the SAXS experiments were carried out at room temperature where the zone formation progresses, even if only to some extent, during the 45 min needed for a measurement.

Most of these disturbing effects can be avoided by the *in situ* measurement of the I.I. in the modified Kiessing type camera. The volume fraction of G.P. zones and/or precipitates formed during the decomposition of the solid solution state of the alloy was determined by numerical integration of the intensity distribution function, and by the *in situ* measurement of the change of the I.I. in the small-angle range. The values obtained by the *in situ* measurements were finally compared and calibrated with the volume fraction values obtained by the integration of the absolute intensity distribution function measured after long-term ageing.

3. Results

The changes in the electrical resistivity obtained during ageing at different temperatures between

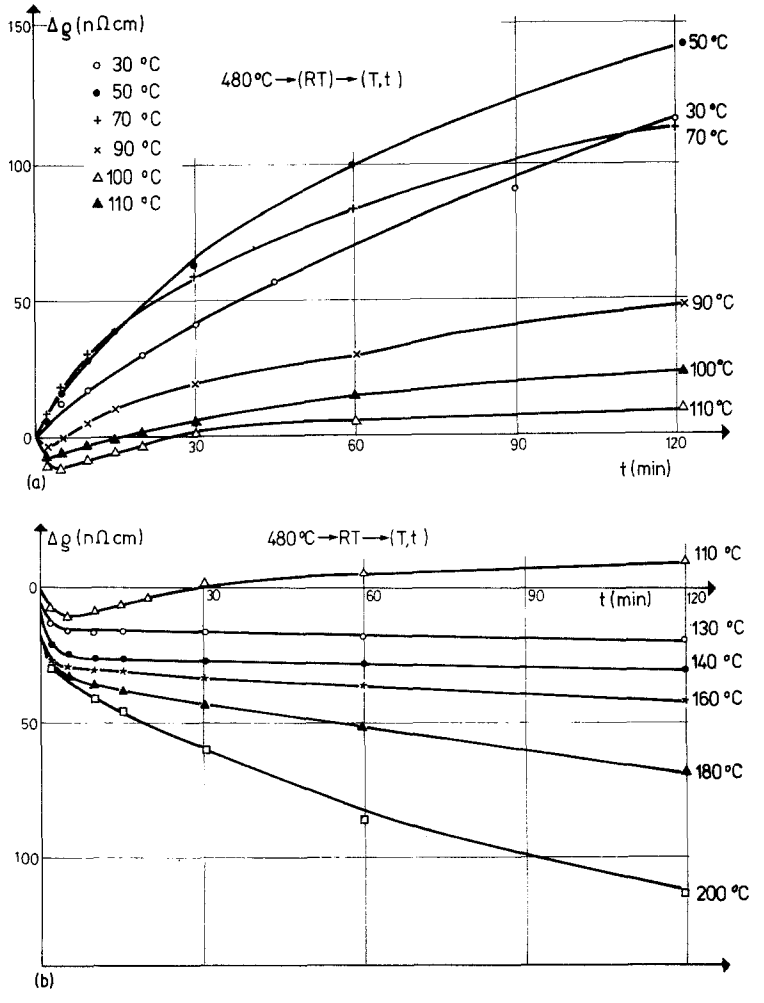

Figure 1 (a) and (b) The change in electrical resistivity as a function of time at different ageing temperatures.

30 and 200° C are shown in Fig. 1a and b. The samples were solution heat-treated at 480° C and quenched into water at room temperature. A time period of 1 min elapsed at room temperature before ageing began. A monotonic increase in the resistivity can be observed during ageing between 30 and 70° C, the rate of which is greatest at the beginning of the ageing process, and is largest after ageing at about 70° C. The greatest resistivity increment, observed within the period of measurement, was obtained, however, at 50° C. At this temperature the resistivity of the alloy increased by 140 nΩ cm within 120 min.

At 90, 100 and 110° C the electrical resistivity of the alloy slightly decreases for a short period of time at the beginning of ageing, and after attaining a minimum, increases monotonically. The resistivity minimum was reached in 2 min at 90° C and in 5 min at 110° C. The value of the resistivity corresponding to the minimum, decreases with increasing temperature, although even at 110° C it is only 10 nΩ cm. The rate of resistivity increment following the minimum decreases with increasing temperature of ageing.

At 130° C and above, no resistivity increment was found, which indicates that at these temperatures there is no, or only a negligible, formation of G.P. zones. In the temperature range between 130 and 160° C, during the first 2 min of ageing, a rather fast process takes place resulting in a considerable decrement of resistivity, which is then followed by a slow change during further ageing. At the same time, the resistivity decrement increases with higher ageing temperatures.

The character of resistivity change is altered around 180° C. At 180° C and especially at 200° C

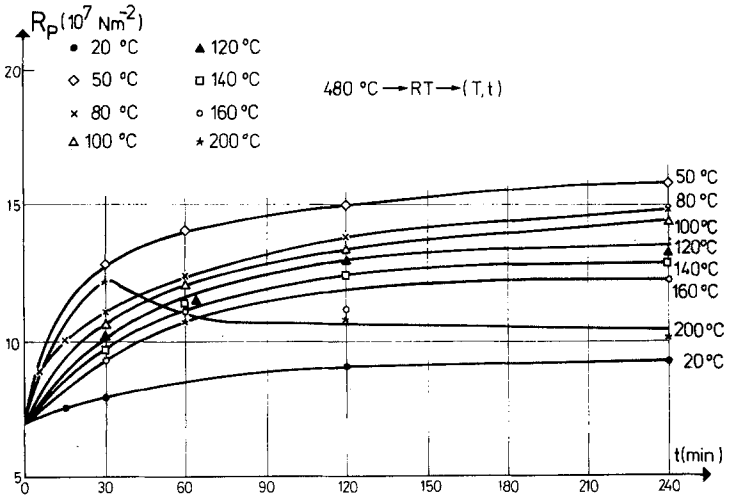

Figure 2 The yield stress as a function of time after ageing at different temperatures.

the resistivity of the alloy decreases with a relatively high rate even during longer periods of ageing. At these temperatures the total decrement of resistivity observed during the entire period of ageing is considerably larger than that measured at 160° C.

The change in the yield stress of samples quenched from 480° C and aged at different temperatures between 20 and 200° C is shown in Fig. 2. The yield stress of the alloy increases monotonically within the 4 h period investigated up to 160° C. At different ageing temperatures, the rate

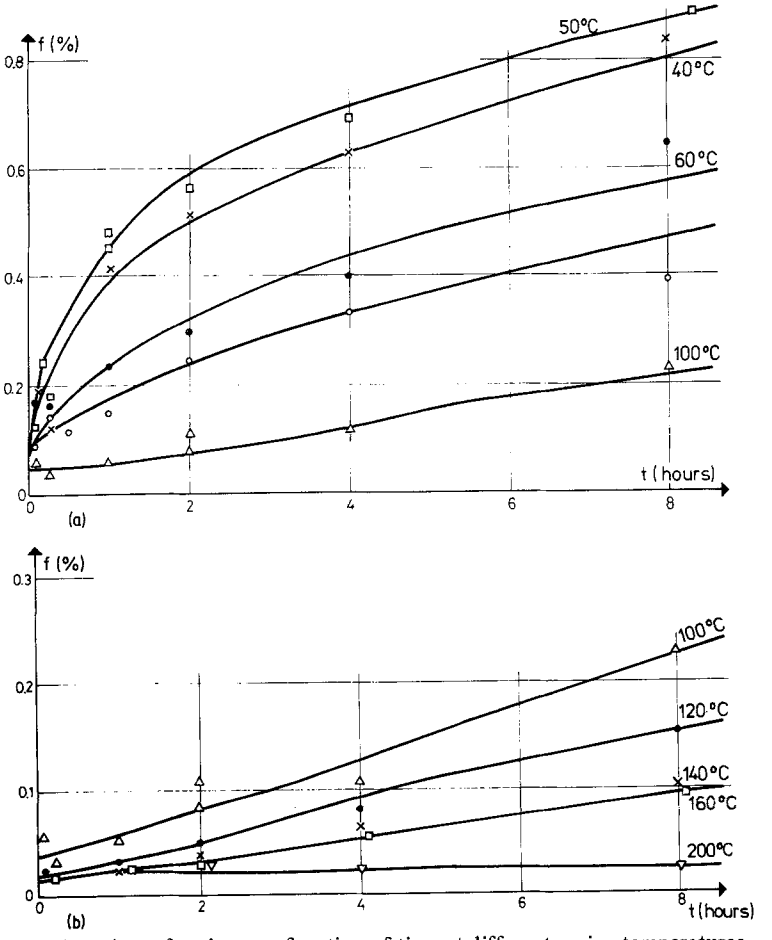

Figure 3 (a) and (b) The volume fraction as a function of time at different ageing temperatures.

of the yield stress increment is largest at the inital stage of ageing and decreases as ageing progresses.

At 20° C, the yield stress of the alloy increases only to a small extent (about 25 MN m^{-2}) during a 4 h ageing period. The largest yield stress increment (90 MN m^{-2}) was observed at 50° C. For ageing between 50 and 160° C, a considerable yield stress increment can be achieved which, however, decreases monotonically with increasing temperature.

The change in the yield stress at 200° C shows a totally different behaviour compared to other ageing temperatures. At this temperature the yield stress increases almost by the same high rate as at 50° C up to about 30 min. After that it decreases, and beyond 120 min it remains practically unchanged.

Fig. 3 shows the changes in the volume fraction of G.P. zones as well as of precipitated particles during ageing at different temperatures for 8 h. The volume fraction of the particles of the second phase in the alloy was determined from the integral intensity of the SAXS intensity distribution curves method [10]. The Zn concentration within the particles was assumed to increase with ageing temperature. The data used were taken from the work of Dünkeloh *et al.*, and are given in Table I.

TABLE I

T (°C)	C_p^{Zn} (at.%)	T (°C)	C_p^{Zn} (at.%)
20	41	60	46
40	43	80	51
50	44	100	56

The Zn concentration in the particles formed during ageing at temperatures above 110° C was assumed to be 66 at.% according to $MgZn_2$ composition of the η' as well as the η particles [1, 5, 7].

The growth of the volume fraction at different

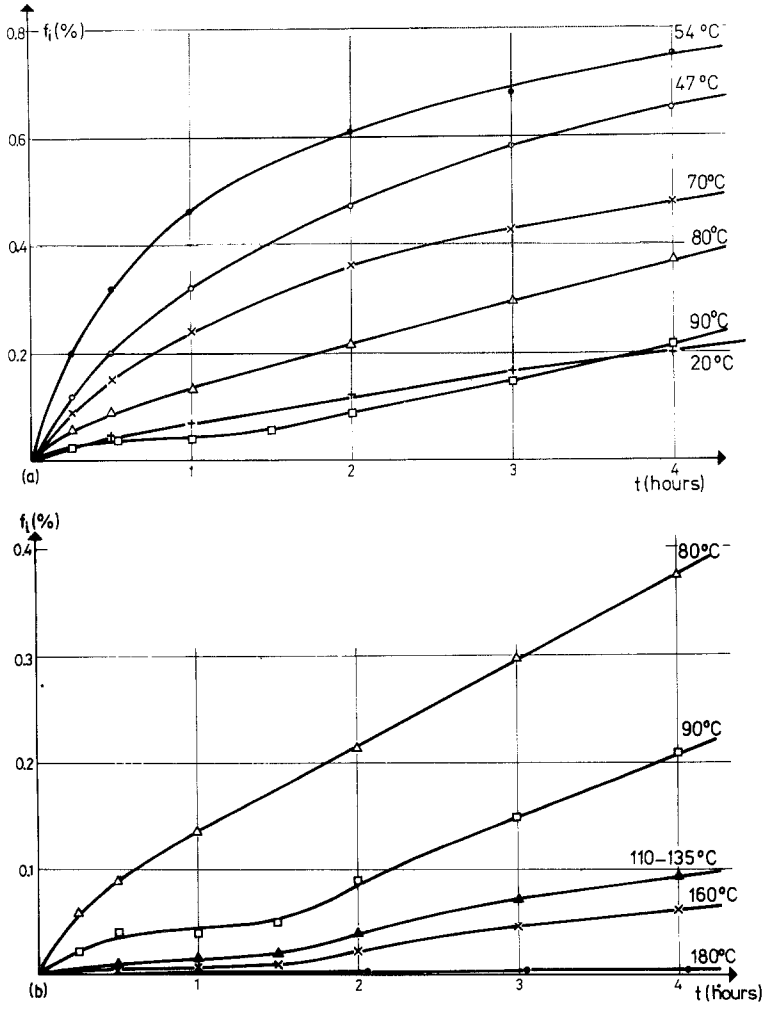

Figure 4 (a) and (b) The change in volume fraction measured *in situ* at different ageing temperatures.

ageing temperatures was also measured *in situ* as mentioned previously. The results of the isothermal measurements are given in Fig. 4. It can be seen from Figs. 3 and 4 that the changes in volume fraction measured by the different techniques are in good agreement.

Growth of the volume fraction at 20° C is rather small within the ageing period of 8 h. A considerably larger increment was observed at 40 and 50° C where it attained 0.8% within the same period of time. At the other ageing temperatures the growth of the volume fraction was always smaller than 0.8%. The values of volume fraction obtained after ageing for 8 h decrease with increasing temperature between 50 and 200° C.

Previous SAXS experiments carried out at room temperature and on the same alloy [8] have revealed a characteristic bump with a second inflexion in the intensity distribution curves (IDC). The present investigations have shown that the IDCs are of the same kind when ageing is carried out at temperatures below 100° C. A Guinier plot evaluation of the IDCs indicated that there are two straight sections in the logarithmic plot, in the region where Guinier approximation is still valid. Similar behaviour of the IDCs was observed by other authors in the Al–Zn–Mg ternary alloy system [13]. On the basis of these results it was assumed that two radii of gyration, R_1 and R_2, are characteristic of the state of the alloy when the bump appears in the IDC (R_1 being the Guinier radius of zones with larger dimensions and R_2 of those with smaller average dimensions).

There is physical evidence for the existence of two different types of G.P. zones in the Al–Zn–Mg alloy system. Ryum carried out multiple-step ageing procedures on an alloy similar to that investigated here. He concluded from hardness measurements that two different types of G.P. zones existed around room temperature [6].

Figs. 5 and 6 show the changes in R_1 and R_2 as a function of ageing time at different temperatures.

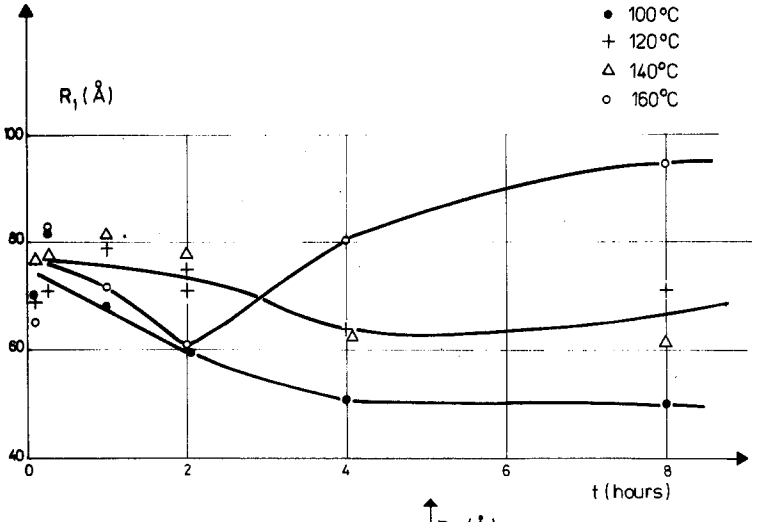

Figure 5 The change of R_1, the Guinier radius, of zones with larger average dimensions as a function of time and temperature.

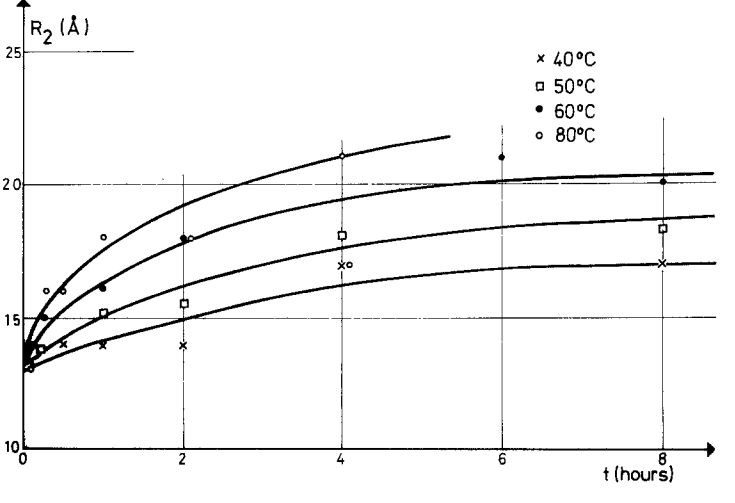

Figure 6 As in Fig. 5 for R_2.

For ageing temperatures higher than 100° C only one straight line can be fitted to the Guinier plot of the IDCs. This means that the particles of the second phase being formed at such temperatures are characterized by only one length parameter. The G.P. zones formed at these temperatures are probably less coherent with the matrix than those formed around room temperature [1, 5]. At the same time, formation of particles of the η' transistion phase which are semicoherent to the matrix also takes place at these temperatures. [14]. As will be shown later, there is direct evidence that G.P. zones and particles of the η' phase co-exist in this transition temperature range between about 100 and 120° C. In this temperature range, the logarithmic analysis of the IDCs reveals only one characteristic length of the particles and the corresponding Guinier radius is denoted by R_1.

Fig. 5 shows the change in R_1 with ageing time and temperature. At 100° C R_1 decreases monotonically which indicates that considerable nucleation of new particles takes place throughout the whole ageing period at this temperature. At 120 and 140° C, except at the very beginning of ageing, R_1 first decreases and finally remains practically constant for longer ageing periods. At 160° C the growth of particles overcomes the rate of nucleation and therefore at longer ageing periods the average dimension of the particles is greater than at 100° C.

R_2, the Guinier radius of the G.P. zones with smaller average diameters, increases monotonically between 40 and 80° C within the time period investigated. Its value is between 13 and 14 Å at the onset of the ageing and increases to 17 to 21 Å over 8 h. The increment is larger at higher ageing temperatures.

The change in the average number, n, of particles is given in Fig. 7. The values of n were calculated assuming that the particles are spherical with a radius $R = (3/5)^{1/2} R_g$, where R_g is the Guinier radius.

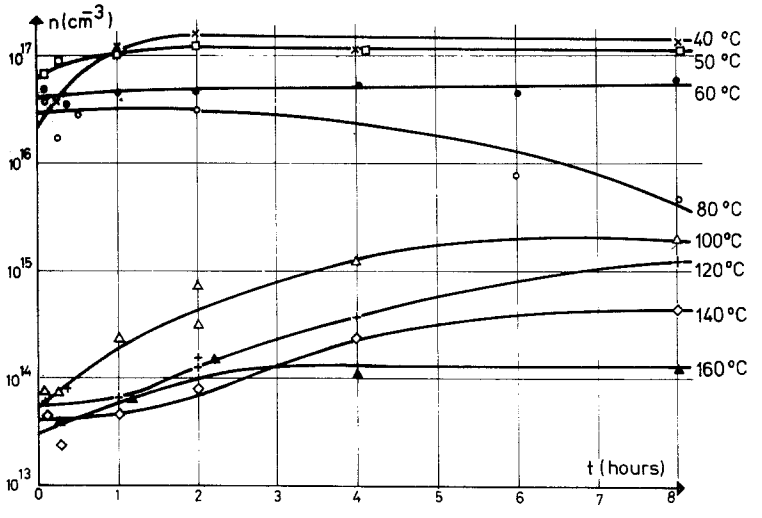

Figure 7 The average number of particles, n, as a function of ageing time and temperature.

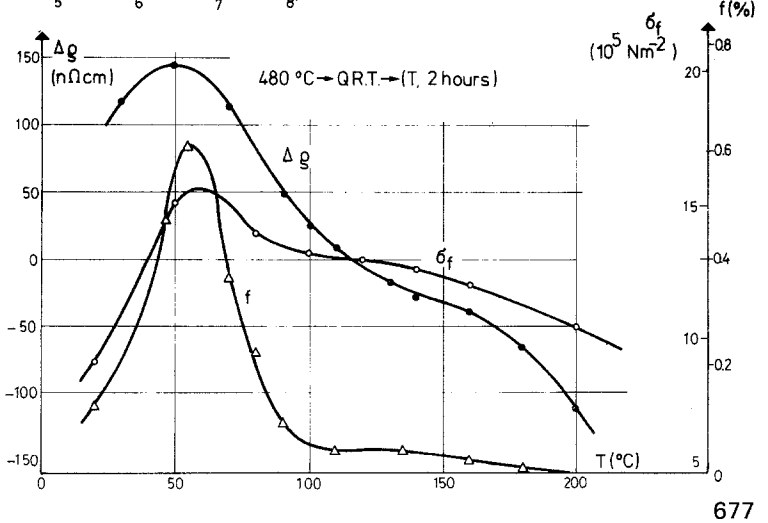

Figure 8 The volume fraction, yield stress and electrical resistivity as a function of temperature after 2 h ageing.

Fig. 8 shows the values of volume fraction, yield stress and electrical resistivity obtained by 2 h ageing at different temperatures. It can be seen that all three quantities show a similar behaviour as a function of temperature: they attain a maximum between 50 and 60° C and quickly decrease at higher temperatures. The change in the electrical resistivity becomes zero at about 115° C and is negative at higher temperatures. The rate of decrement of the electrical resistivity becomes considerably larger at temperatures above 160° C.

4. Discussion

Several investigations have shown that in the Al–Zn–Mg type alloys investigated here the decomposition of the super-saturated solid solution state takes place by the formation of G.P. zones in the temperature range between room temperature and 100° C [1, 7, 15]. On the other hand, between 140 and 200° C, the basic process which eliminates the solid solution state is the formation of the η' transition, the Zn_2Mg type and to some extent the formation of the T phase [1–9].

On the basis of these investigations, three temperature ranges can be defined in the decomposition process of the solid solution state, in the alloy studied here. Between room temperature and about 70° C the basic process is the nucleation and growth of G.P. zones. This is indicated by the simultaneous and monotonic increase observed in the electrical resistivity volume fraction and yield stress of the alloy.

A transition temperature range can be observed between about 80 and 110° C. A small decrease in electrical resistivity can be observed at the onset of ageing (see Fig. 1). The behaviour of the growth kinetics of the volume fraction changes in this temperature range as can be seen in Fig. 3b: the growth kinetics of the volume fraction appear to be of a logarithmic type at 50° C, whereas they are approximately linear at 80° C. At the same time, it should be noted that the yield stress exhibits the same behaviour in this transition temperature range as at lower temperatures.

The transition nature of this temperature range is further indicated by the growth kinetics of the volume fraction at temperatures above 90° C where it shows a definite incubation period at the beginning of ageing (see Fig. 4). At the same temperatures, and for the same periods of ageing, the yield stress increases monotonically. This means that in this temperature range a process takes place which improves the yield stress but leaves the SAXS in the alloy unchanged.

This effect can be explained if the fact that the alloy contains 0.25 wt % Si is taken into account, and that the formation of the β' type Mg_2Si phase takes place exactly in this temperature range in an Al–Mg–Si alloy [16, 17]. Under similar conditions, this effect was not observed on alloys with no Si content. Therefore, it can be concluded that between 110 and 160° C β' type particles are also formed as well as particles of the η' phase. The electrical resistivity is reduced by both types of particle, whereas only the η' phase particles produce the SAXS effect.

At 180° C and above, a strong resistivity decrement can be observed, but no SAXS effect is obtained. This is clear if we take into account that at these temperatures particles of the η phase are formed which can grow to several hundred angstroms. At the same time, the particles of the η' phase can also rapidly attain a size of a few hundred

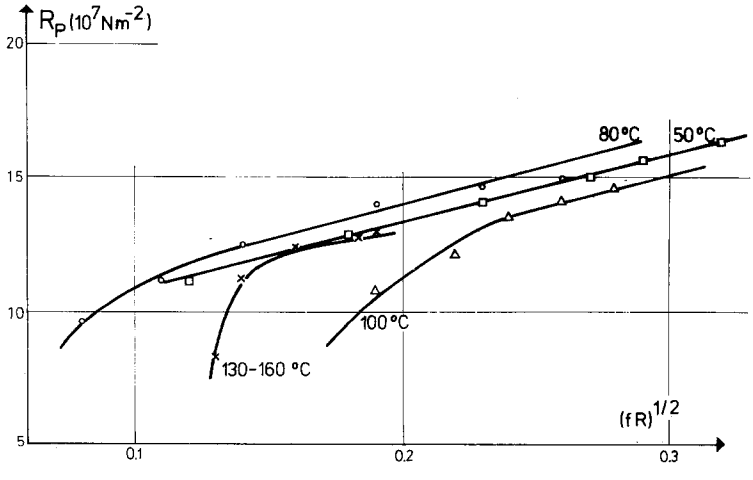

Figure 9 Correlation between the yield stress and $(fR)^{1/2}$.

angstroms after quenching at these temperatures [3, 4, 6, 9, 18]. These large particles cause a considerable resistivity decrement but are larger, on average, than the largest particle size which can be observed by the present SAXS apparatus. A strong coarsening of the precipitate particles is also indicated by the yield stress–ageing time curve at 200° C in Fig. 1.

Earlier reversion experiments carried out on the same type of alloy have shown that hardening takes place by the intersection mechanism [9]. According to this, the yield stress must be a linear function of $(fR)^{1/2}$, where R is the average radius and f the volume fraction of the particles. This correlation is given in Fig. 9 for ageing at 50, 80, 100 and 140° C. It can be seen that the plot is linear for 50 and 80° C, and the specific surface energy necessary to cut a G.P. zone by a dislocation may be calculated from the slope of the line. It was found to be $\Gamma_0 = 0.21\,\mathrm{N\,m\,m^{-2}}$, which is in good agreement with our earlier results [9] taking into account that in the previous calculation the conversion factor of 3 between tensile stress, σ and the resolved shear stress, τ $(3\tau = \sigma)$, was not included.

Fig. 9 also shows that at higher temperatures the yield stress is by no means proportional to $(fR)^{1/2}$ and the discrepancy increases at higher temperatures. This behaviour is in good agreement with the model given for the decomposition process at temperatures above 90° C.

Above 100° C, the appearance of the β' type Mg_2Si particles causes non-proportionality of the yield stress and $(fR)^{1/2}$.

References

1. H. SCHMALZRIED and V. GEROLD, *Z. Metallkd.* **49** (1957) 291.
2. J. L. TAYLOR, *J. Inst. Metals* **92** (1963) 301.
3. J. D. EMBURY and R. B. NICHOLSON, *Acta Met.* **13** (1965) 403.
4. G. W. LORIMER and R. B. NICHOLSON, *ibid.* **14** (1966) 1009.
5. K. H. DÜNKELOH, G. KRALIK and V. GEROLD, *Z. Metallkd.* **65** (1974) 291.
6. N. RYUM, *ibid.* **66** (1975) 338.
7. L. F. MONDOLFO, *Met. Rev.* **153** (1971) 95.
8. G. GROMA, E. KOVÁCS-CSETÉNYI, I. KOVÁCS, J. LENDVAI and T. UNGÁR, *Z. Metallkd.* **67** (1976) 404.
9. T. UNGÁR, J. LENDVAI, I. KOVÁCS, G. GROMA and E. KOVÁCS-CSETÉNYI, *Z. Metallkd.* **67** (1976) 683.
10. H. BRUMBERGER, (Ed.), Proceeding of the Conference on X-Ray Small Angle Scattering, (Gordon and Breach, New York, 1966).
11. T. UNGAR, to be published.
12. O. KRATKY, I. PILZ and P. J. SCHNITZ, *J. Colloid and Interface Sci.* **21** (1966) 24.
13. M. MURAKAMI, O. KAWANO and Y. MURAKAMI, *Acta Met.* **17** (1969) 29.
14. L. F. MONDOLFO, *J. Inst. Met.* **97** (1969) 95.
15. R. GRAF, *Compt. Rend. Acad, Sci. Paris* **242** (1965) 1311; **244** (1967) 337.
16. D. W. PASHLEY, J. W. RHODES and A. SENDOREK, *J. Inst. Metals* **94** (1966) 41.
17. M. H. JACOBS, *Phil. Mag.* **26** (1972) 1.
18. I. KOVÁCS, J. LENDVAI, T. UNGÁR, K. BANIZS and J. LAKNER, *Aluminium* **53** (1977) 497.

Received 17 May and accepted 20 July 1978.